8188 *Inorg. Chem.* **2010**, *49*, 8188–8190
DOI: 10.1021/ic100795p

Inorganic Chemistry
Communication

Catalytically Stable and Active CeO_2 Mesoporous Spheres

Xin Liang,[†,‡] Junjia Xiao,[†] Biaohua Chen,[†] and Yadong Li*[,§]

[†]*State Key Laboratory of Chemical Resource Engineering, Beijing University of Chemical Technology, Beijing 100029, People's Republic of China, and* [§]*Department of Chemistry, Tsinghua University, Beijing 100084, People's Republic of China.* [‡]*Tel: +86-10-64412054. Fax: +86-10-64419619. E-mail: liangxin@mail.buct.edu.cn.*

Received April 23, 2010

A facile one-step strategy has been developed for preparing monodisperse CeO_2 mesoporous spheres with high surface areas, uniform size distributions, and well-defined pore topologies. These mesoporous spheres have been demonstrated to be catalytically stable and active for CO oxidation.

Ceria is a useful promoter and an important component for three-way catalysts because of its unique redox properties, strong oxygen storage, and release capability via facile conversion between Ce^{3+} and Ce^{4+} oxidation states.[1−3] Researchers have discovered that the catalytic performance of CeO_2 materials has been greatly influenced by their structural properties, such as surface area, naked crystal planes, and surface states.[4−6] CeO_2 mesoporous spheres have been of increasing interest in catalysis for their unique structural properties, such as high surface area, special interfaces, uniform size distribution, and well-defined pore topology. The penetrable shells allow the diffusion of chemical reagents toward the inside of the structure, the high surface area is helpful for the high metal dispersion, and the pore channels help in the adsorption and desorption of reactants and increase the effectiveness of the contact between catalysts and reactants. Thus, CeO_2 mesoporous spheres with narrow pore distributions, high surface areas, well-defined morphologies, and rigid frameworks should have great advantages in confined-space and environmental catalysis.[7−9]

For the construction of CeO_2 mesoporous materials, the most common approach is the use of hard or soft sacrificial templates.[10−15] For example, Corma and co-workers have synthesized mesostructured CeO_2 materials using CeO_2 nanoparticles as starting materials and a $EO_{20}PO_{70}EO_{20}$ triblock copolymer as the soft template.[9] Stucky and co-workers used MCl_n as the metal source and poly(ethylene oxide)-based triblock copolymers as soft templates in an ethanolic solution to synthesize mesoporous metal oxides.[15,16] CeO_2 mesoporous materials have been synthesized by using SBA-15 and KIT-6 as sacrificial templates.[17] However, there are limited reports for the direct and template-free synthesis of CeO_2 mesostructures, especially mesostructures with narrow pore distributions, rigid frameworks, and well-defined morphologies until now. Developing an effective, direct, and template-free synthetic approach for CeO_2 mesostructures is desirable.

Herein, a reproducible and one-step synthetic strategy has been developed for preparing nearly monodisperse CeO_2 mesoporous spheres using simple inorganic salt $Ce(NO_3)_3 \cdot 6H_2O$ and organic acids C_2H_5COOH as starting materials without any other complex surfactants. Under the designed conditions, uniform CeO_2 mesoporous spheres with high surface areas, well-defined morphologies, narrow size distributions, and good thermal stability could be obtained in large quantities.

In a typical synthesis, 1.0 g of $Ce(NO_3)_3 \cdot 6H_2O$ was dissolved in 1 mL of deionized water. Then, 1 mL of C_2H_5COOH and 30 mL of glycol were added with stirring to form a uniform solution. The mixed solution was sealed and heated at 180 °C for 200 min to get the products. Transmission electron microscopy (TEM) images of the products (Figure 1a−c) showed that the samples were spheres with

*To whom correspondence should be addressed. E-mail: ydli@tsinghua.edu.cn. Tel: +86-10-62772350. Fax: +86-10-62788765.

(1) Trovarelli, A. *Catal. Rev. Sci. Eng.* **1996**, *38*, 439.
(2) Kaspar, J.; Fornasiero, P.; Graziani, M. *Catal. Today* **1999**, *50*, 285.
(3) Rodriguez, J. A.; Hanson, J. C.; Kim, J. Y.; Liu, G.; Iglesias-Juez, A.; Fernandez-Garcia, M. *J. Phys. Chem. B* **2003**, *107*, 3535.
(4) Zhou, K. B.; Wang, X.; Sun, X. M.; Peng, Q.; Li, Y. D. *J. Catal.* **2005**, *229*, 206.
(5) Guzman, J.; Carrettin, S.; Corma, A. *J. Am. Chem. Soc.* **2005**, *127*, 3286.
(6) Carrettin, S.; Concepcion, P.; Corma, A.; Nieto, J. M. L.; Puntes, V. F. *Angew. Chem., Int. Ed.* **2004**, *43*, 2538.
(7) Lyons, D. M.; Ryan, K. M.; Morris, M. A. *J. Mater. Chem.* **2002**, *12*, 1207.
(8) Yuan, Q.; Liu, Q.; Song, W. G.; Feng, W.; Pu, W. L.; Sun, L. D.; Zhang, Y. W.; Yan, C. H. *J. Am. Chem. Soc.* **2007**, *129*, 6698.
(9) Corma, A.; Atienzar, P.; García, H.; Ching, J. Y. C. *Nat. Mater.* **2004**, *3*, 304.
(10) Terribile, D.; Trovarelli, A.; Llorca, J.; Leitenburg, C.; Dolcetti, G. *J. Catal.* **1998**, *178*, 299.
(11) Pavasupreea, S.; Suzukia, Y.; Pivsa-Artb, S.; Yoshikawa, S. *J. Solid State Chem.* **2005**, *178*, 128.
(12) Terribilea, D.; Trovarellia, A.; Llorcab, J.; Leitenburga, C.; Dolcettia, G. *Catal. Today* **1998**, *43*, 79.
(13) Yuan, Q.; Liu, Q.; Song, W. G.; Feng, W.; Pu, W. L.; Sun, L. D.; Zhang, Y. W.; Yan, C. H. *J. Am. Chem. Soc.* **2007**, *129*, 6698.
(14) Sinha, A.; Suzuki, K. *J. Phys. Chem. B* **2005**, *109*, 1708.
(15) Fan, J.; Boettcher, S. W.; Stucky, G. D. *Chem. Mater.* **2006**, *18*, 6391.
(16) Mak, A.; Yu, C.; Yu, J.; Zhang, Z.; Ho, C. *Nano Res.* **2008**, *1*, 474.
(17) Rossinyol, E.; Arbiol, J.; Peiró, F.; Cornet, A.; Morante, J. R.; Tianb, B.; Bob, T.; Zhao, D. *Sens. Actuators B* **2005**, *109*, 57.

 Published on Web 08/20/2010

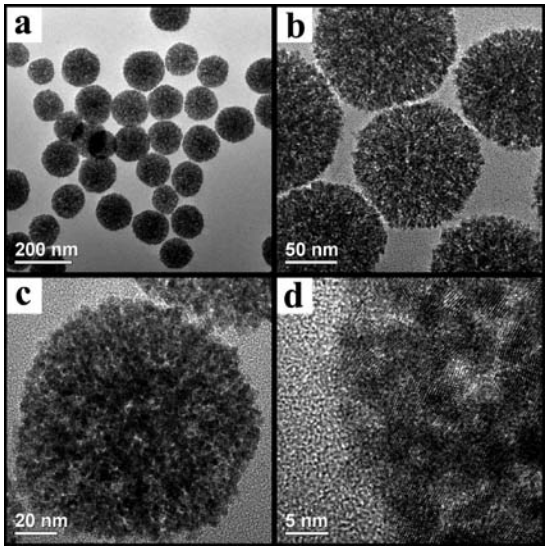

Figure 1. (a−c) Typical TEM images of CeO_2 mesoporous spheres with different magnifications. (d) HRTEM image of the CeO_2 mesoporous sphere.

narrow size distributions and an average size of 130 nm. It can be seen from the high-resolution TEM (HRTEM) image (Figure 1d) that the spheres are comprised of many small particles with a crystallite size of 3−5 nm, and there are clear voids with diameter 3−5 nm among the small particles, revealing the mesostructure of the CeO_2 spheres. X-ray diffraction (XRD) patterns of the samples (Figure S3 in the Supporting Information, SI) clearly show that all of the peaks can be indexed as arising from the pure phase of face-centered-cubic CeO_2 (JCPDS 65-2075). The crystallite size estimated by the Scherrer equation from the width of the strongest (111) line in the XRD pattern is 3.7 nm, which corresponds well with the crystallites size measured from the HRTEM micrographs.

The formation process of the CeO_2 mesoporous spheres was demonstrated to be well-assisted with a two-stage growth model.[18,19] As shown in Figure 2, in the first stage, the Ce^{3+} ions hydrolyzed and were oxidized by NO_3^- to form CeO_2 nanosized crystalline precursors in a supersaturated solution under solvothermal conditions. Then, in the second stage, the initially formed small particles self-assembled into larger secondary particles. Ethylene glycol can be absorbed on the surface of the nanosized crystalline precursors. On the other hand, propanoic acid could react with ethylene glycol by esterification, which enlarged the surface modification effect of these small molecules on the surface state. Gas chromatography−mass spectrometry (GC−MS) analysis of the reaction media confirmed the formation of the ester (Figure S9 in the SI). Ethylene glycol and ester act as structure-directing agents to regulate the surface state of the nanosized precursors, further influence the nucleation and aggregate process of the nanoparticles, and finally lead to the formation of mesoporous structures.

Experiments have shown that these CeO_2 mesoporous spheres could not form in the absence of propanoic acid. As discussion above, the surface modification effect of propanoic acid would be the key effect leading to the formation of

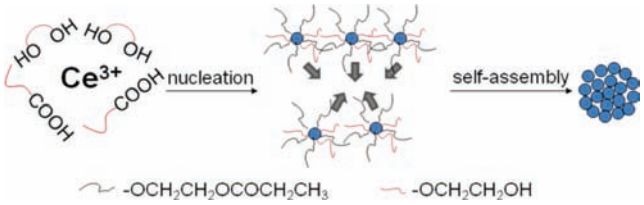

Figure 2. Illustration of the formation process of CeO_2 mesoporous spheres.

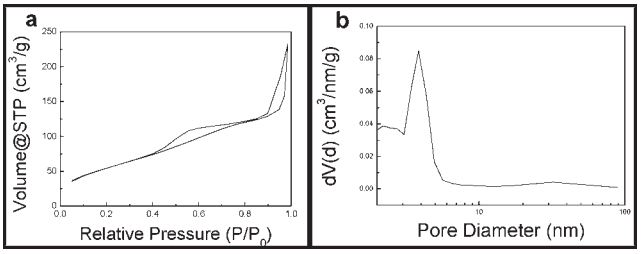

Figure 3. (a) N_2 adsorption and desorption isotherms of CeO_2 mesoporous spheres. (b) BJH pore size distribution curves of CeO_2 mesoporous spheres.

these mesoporous spheres. Therefore, other organic acids with similar structures and groups would also lead to the formation of mesoporous structures. By using CH_3COOH and n-C_3H_7COOH instead of propanoic acid, similar CeO_2 mesoporous spheres have been obtained (Figure S4 in the SI), sustaining the growth mechanisms to some extent.

The textural porosities of the mesoporous spheres were examined by N_2 adsorption and desorption analysis. The N_2 adsorption and desorption isotherms and mesopore size distribution plots for CeO_2 mesoporous spheres are given in Figure 3. CeO_2 mesoporous spheres have high surface areas (S_{BET} = 216 m^2/g). CeO_2 mesoporous spheres displayed a type IV N_2 adsorption/desorption isotherm, implying the mesostructure. CeO_2 spheres have an obvious strong and narrow peak at about 3.8 nm calculated by Barrett−Joyner−Halenda (BJH) analysis using the desorption branch of the isotherm, proving that the spheres have narrow pore size distributions. The results are well consistent with HRTEM and XRD analysis. Besides the well-defined mesopores, CeO_2 mesospheres showed interparticle porosity, which was evidenced by the adsorption step at high relative pressures (> 0.8).

Thermal stability is an important evaluation criterion for catalysts. Figure S5 in the SI displays TEM images of the CeO_2 mesoporous spheres calcined at 300 and 500 °C. It can be seen that the morphology of CeO_2 mesoporous spheres remained well under the annealing temperature of 500 °C, revealing the good thermal stability of the CeO_2 mesoporous spheres. All of the samples have type IV N_2 adsorption/desorption isotherms, confirming the mesopore structures (Figure S6 in the SI). The Brunauer−Emmett−Teller (BET) surface area of CeO_2 mesoporous spheres exhibits no significant change under different annealing temperatures (204 m^2/g at 300 °C and 199 m^2/g at 500 °C). From the pore size distribution plots, it can be seen that the pore size distributions are almost the same for the samples without annealing and with annealing at 300 °C. There are strong and narrow peaks in the region of 3−5 nm. For the samples annealed at 500 °C, there is still a strong peak in the region of 3−5 nm. The intensity of the wide peak corresponding to the internanparticle porosity at 30 nm increased, revealing that

(18) Ge, J. P.; Hu, Y. X.; Biasini, M.; Beyermann, W. P.; Yin, Y. D. *Angew. Chem., Int. Ed.* **2007**, *46*, 4342.
(19) Libert, S.; Gorshkov, V.; Goia, D.; Matijevi, E.; Privman, V. *Langmuir* **2003**, *19*, 10679–10683.

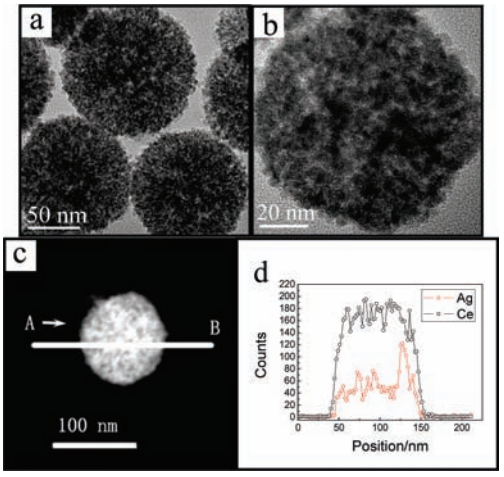

Figure 4. (a and b) TEM images with different magnifications of CeO_2 mesoporous spheres supported by a Ag nanoparticle catalyst. (c) Dark-field scanning TEM image of a single CeO_2 mesoporous sphere. (d) Compositional line profile across the single sphere (from A to B) probed by EDXA line scanning.

the CeO_2 mesoporous spheres slightly aggregate with each other during calcination at relatively high temperature.

The narrow pore distributions, high surface areas, good adsorbabilities, and relatively high thermal stabilities endow the CeO_2 mesoporous spheres as great candidates for catalyst support to construct catalytically active and stable nanoreactors compared with other morphologies. Monodisperse Ag nanoparticles were selected to be doped in CeO_2 mesoporous spheres to demonstrate the catalytic performance of CeO_2 mesoporous spheres based on nanoreactors for their relatively low cost compared with other noble metal catalysts. CeO_2 mesoporous spheres have shown high absorbability for monodisperse Ag nanoparticles. By the simple addition of CeO_2 mesoporous spheres into a monodisperse Ag nanoparticles colloid with stirring, the Ag nanoparticles were readily and rapidly absorbed by the CeO_2 mesoporous spheres (Figure S7 in the SI). TEM images of the CeO_2 mesoporous spheres absorbed by Ag nanoparticles are displayed in Figure 4a,b. It can be seen that there are all spheres in the image, which reveals that Ag nanoparticles were completely absorbed in the mesopores of the CeO_2 spheres. Elemental analysis was carried out by an energy-dispersive X-ray analysis (EDXA) line scanning across a single sphere, which confirmed the existence and the good dispersity of Ag nanoparticles in the mesoporous spheres (Figure 4c,d). These CeO_2 mesoporous spheres have also shown good absorbability for Au nanoparticles (Figure S8 in the SI), revealing that these CeO_2 mesoporous spheres were good supports for various metal nanoparticles to construct novel catalytically nanoreactors.

The CO oxidation reaction was selected as a model reaction to examine the catalytic performance of the as-prepared nanoreactors. The conversion profiles of CO versus temperature results are shown in Figure 5, revealing the excellent performance of CeO_2 mesospheres and CeO_2 mesosphere-based nanoreactors for CO oxidation. T_{90} of the undoped CeO_2 mesoporous spheres is 330 °C. Compared with the

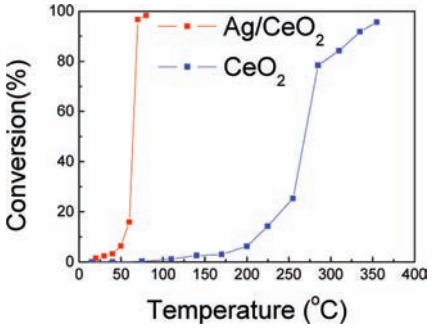

Figure 5. Catalytic performance of CeO_2 mesoporous spheres for CO oxidation.

undoped CeO_2 spheres, the Ag/CeO_2 spheres (Ag molar content 10%) are more active for CO oxidation. The conversion−temperature curve revealed that the catalyst is temperature-sensitive for the CO oxidation reaction. At a narrow temperature interval, the percentage of CO conversion increased from 10% at 55 °C to 90% at 68 °C. At 70 °C, the percentage of CO conversion was 96.5% over Ag-doped CeO_2 spheres. The results are better than some reported data.[20,21] Compared with other morphologies, such as nanorods and nanoparticles, the CeO_2 mesoporous spheres show superior catalytic properties (Figure S10 in the SI).

In conclusion, we have developed an effective method for the fabrication of CeO_2 mesoporous spheres. Only small molecular organic acids were used as structure-directing agents without any other complex surfactants. This novel synthetic strategy should offer good suggestions for other kinds of metal oxide mesoporous sphere systems, such as rare earth oxides, and so on. Because CeO_2 are useful materials for catalysis, these mesoporous CeO_2 spheres have great potential in the field of confined-space and environmental catalysis for their high surface areas and unique porosity structures. It was demonstrated that mesoporous CeO_2 spheres have of excellent catalytic performance for the CO oxidation reaction compared with the reported results. These CeO_2 mesoporous spheres should be good candidates for catalyst support to construct catalytically stable and active nanoreactors in the field of confined-space and environmental catalysis.

Acknowledgment. This work was supported by NSFC (Grant 90606006), the Foundation for the Author of National Excellent Doctoral Dissertation of China and the State Key Project of Fundamental Research for Nanoscience and Nanotechnology (Grant 2006CBON0300), and the Chinese Universities Scientific Fund (Grant QN0903).

Supporting Information Available: Experimental details, N_2 adsorption and desorption analysis, TEM images, XRD patterns, GC−MS analysis of the reaction media, and catalytic performance of the reference samples. This material is available free of charge via the Internet at http://pubs.acs.org.

(20) Imamura, S.; Yamada, H.; Utani, K. *Appl. Catal., A* **2000**, *192*, 221.
(21) Lundberg, M.; Skårman, B.; Wallenberg, L. R. *Microporous Mesoporous Mater.* **2004**, *69*, 187.